Analysis and Simulation of a Digital Matched Filter Receiver of Pseudo-Noise Signals

Abstract: This paper discusses the performance of a digital matched filter receiver matched to a biphase-modulated signal in a clutter environment consisting of other biphase-modulated signals. Analytic results for a white-Gaussian model and for a non-linear capture model are compared with simulation results obtained from an IBM 7094 computer. The white-Gaussian model is in general agreement with the simulation results for equal power clutter signals; the capture model and the simulator yield similar results when a dominant clutter source is present.

Introduction

In this paper the performance of a digital matched filter for the reception of pseudo-noise, biphase-modulated signals is analyzed. A simulation of this filter on a general-purpose computer is also discussed. The radio receiver described by Corr, et al. utilized digital matched filters similar to those analyzed in this paper. However, here the emphasis will be placed on the performance of a receiver containing components that perform in an "ideal" manner. The discussion treats the performance of the digital matched filter in an environment that contains the signal to which the filter is matched and other similar signals (clutter) to which the filter is not matched. The effects of thermal noise and band limiting operations which distort the instantaneous phase shifts of the biphase modulation are neglected.

The matched filter operation is performed on the bandpass signal by first generating baseband quadrature components and then performing two baseband matched filter operations. Figure 1 gives a block diagram of such a matched filter.

The clutter problem is treated first from a white noise viewpoint based on the approach used for analog matched filters,² and then strong clutter sources are considered from a non-Gaussian point of view. In the strong clutter analysis the nonlinear effects of hard limiting are included.

Finally, the performance of the filter combined with either a "greatest of" or a "threshold" detector is discussed and simulation results are presented.

Analysis of digital matched filter performance

The purposes of this section are to give insight into the performance of a digital matched filter and to establish a basis for interpreting the results of the simulation. The first part of this section is included as an explanation of the filter mechanism; nonlinear effects are not given. A short discussion of the performance of the filter under the assumption of a white-Gaussian environment is included. The output signal-to-noise ratio is calculated so that the results of Turin, Reiger, and Nuttall for the error rate versus output signal-to-noise ratio of an analog matched filter with an M-ary signal alphabet can be compared with the simulation results for a digital matched filter. A nonlinear capture model is also developed to explain the results of the simulation when a dominant clutter signal is present.

The received signal is of the form

$$s(t) = \sum_{i=1}^{K} s_i(t) = \sum_{i=1}^{K} A_i \cos \{\omega_0(t - \Delta_i) + \theta_i + \psi_i(t - \Delta_i)\}, \quad 0 < t < T$$
 (1)

where

 A_i = amplitude of the i^{th} signal at the desired receiver, ω_0 = carrier frequency,

 $\psi_i(t)$ = biphase pseudo-noise modulation (i.e., a sequence of M 0's and π 's) to which the i^{th} receiver is matched,

 θ_i = rf phase of the i^{th} signal,

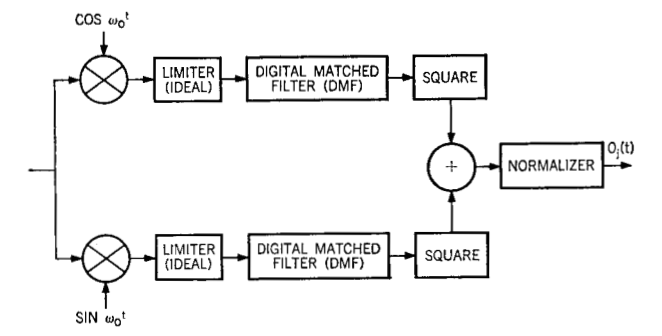


Figure 1 Block diagram of digital matched filter.

T = duration of the modulated rf pulse,

 Δ_i = delay of the i^{th} signal.

After quadrature mixing and lowpass filtering, the signal takes the forms

$$\frac{1}{(\sum A_i^2)^{1/2}} \left[\sum_i A_i \cos \psi_i (t - \Delta_i) \cos \theta_i \right]$$
 (2a)

and

$$\frac{1}{(\sum_{i} A_i^2)^{1/2}} \left[\sum_{i} A_i \cos \psi_i (t - \Delta_i) \sin \theta_i \right]$$
 (2b)

in the cosine and sine arms, respectively (see Fig. 1). The denominator factor $(\sum_i A_i^2)^{1/2}$ is included so that the maximum output of the matched filter will be independent of the input power, i.e., normalized. The nonlinear effects of hard limiting are not considered in this analysis; however, they are included in the analysis of strong clutter sources and in the simulation results given later in this paper. However, it is known⁶ that for white noise, hard limiting will reduce the output signal-to-noise ratio by a few dB. Since each receiver is matched to a different biphase signal, the output of the receiver matched to $\psi_i(t)$ is the sum of the squares of the outputs of the two arms and is given by

$$O_{i}(t) = \frac{1}{\sum_{i} A_{i}^{2}} \left\{ \sum_{\gamma} \cos \psi_{i}(\gamma \delta) \right.$$

$$\left[\sum_{i} A_{i} \cos \psi_{i}(t - \gamma \delta - \Delta_{i}) \cos \theta_{i} \right] \right\}^{2}$$

$$+ \frac{1}{\sum_{i} A_{i}^{2}} \left\{ \sum_{\gamma} \cos \psi_{i}(\gamma \delta) \right.$$

$$\left[\sum_{i} A_{i} \cos \psi_{i}(t - \gamma \delta - \Delta_{i}) \sin \theta_{i} \right] \right\}^{2}. \quad (3)$$

Here δ is the sampling rate of the digital matched filter and \sum_{γ} represents the sum over all stages of the shift register. By interchanging the order of the summations, one can show that

$$O_{i}(t) = \frac{1}{\sum_{i} A_{i}^{2}} \left[\sum_{i} A_{i}^{2} R_{ij}^{2}(t - \Delta_{i}) + 2 \sum_{i \neq k} A_{i} A_{k} R_{ij}(t - \Delta_{i}) R_{kj}(t - \Delta_{k}) \right]$$

$$\times \cos (\theta_{i} - \theta_{k}). \tag{4}$$

Here R_{ij} is the crosscorrelation between the i^{th} and j^{th} signals and R_{ij} is the autocorrelation of the j^{th} signal.

For example, consider the output of receiver 1 in an environment containing the desired signal without interference. Since there are no clutter talkers, Eq. (4) simplifies to the form

$$O_1(t) = R_{11}^2(t - \Delta_i).$$
 (5)

In other words the output is the autocorrelation function of signal 1. At the instant of match, $t = \Delta_1$ and

$$O_1(\Delta_1) = R_{11}^2(0) = 1,$$
 (6)

since R_{11} is the normalized autocorrelation function. In fact, although the output is deterministic, if statistical averaging is performed over the complete set of outputs the results would be the same as the statistics for coin flipping. Specifically, toss a coin n times, where n = number of bits in each arm of the digital matched filter. The output is then given by (heads — tails) $^2/n^2$, which on the average is 1/n.

Now, consider the output of receiver 1 in an environment with the desired signal and a single interfering signal.

$$O_1(t) = \frac{1}{A_1^2 + A_2^2} \left[A_1^2 R_{11}^2 (t - \Delta_1) + A_2^2 R_{21}^2 (t - \Delta_2) \right]$$

$$+ 2 A_1 A_2 R_{11}(t - \Delta_1) R_{21}(t - \Delta_2) \cos(\theta_1 - \theta_2)$$
]. (7)

The first two terms represent the contributions of the separate signals; the third term is a mutual contribution. Since the rf phases of the two signals are independent, the average of the mutual clutter term, $\cos{(\theta_1 - \theta_2)}$, over phase is zero. Hence, the "expected value" of the output averaged over the rf phases is

$$E[O_1(t)] = \frac{1}{A_1^2 + A_2^2} [A_1^2 R_{11}^2 (t - \Delta_1) + A_2^2 R_{21}^2 (t - \Delta_2)].$$
 (8)

At the time of match $t = \Delta_1$:

$$E[O_1(\Delta_1)] = \frac{1}{A_1^2 + A_2^2} [A_1^2 + A_2^2 R_{21}^2]$$

$$= 1 - \frac{A_2^2}{A_1^2 + A_2^2} (1 - R_{21}^2). \tag{9}$$

The time argument of R_{21} has been dropped because the statistics of R_{21} are independent of time. Hence, the output at the time of match is reduced by an amount proportional to the ratio of the clutter power to the total power.

In general, if many clutter sources are present,

$$E[O_1(\Delta_1)] = 1 - \frac{P_e}{P_A + P_e} (1 - R^2), \tag{10}$$

where P_c is the clutter power of those signals that overlap the desired signal, P_o is the signal power, and R^2 is the expected value of the square of the crosscorrelation function.

At all times other than the desired time of match, Eq. (8) yields

$$E[O_1(t)] = R^2, t \neq \Delta_1. (11)$$

Here, $R^2 = R_{11}^2 = R_{21}^2$ since the statistics of R_{11}^2 and R_{21}^2 are identical and essentially independent of time. In general, Eq. (10) holds independent of the number of clutter sources.

• White-Gaussian model

Additional understanding of the digital matched filter can be obtained by considering the signal-to-noise ratio at the output of this system. Here, the clutter will be assumed to have a white-Gaussian distribution and it becomes possible to make use of well known results to determine the output signal-to-noise ratio. For a matched filter in a white-Gaussian noise environment it has been shown that the peak output signal-to-noise ratio η_n^2 is given by

$$\eta_p^2 = \frac{2E}{N_{0.T}},\tag{12}$$

where E is the signal energy and N_{0T} is the total Gaussian noise power density. The simulation discussed later shows that the white-Gaussian assumption is valid for digital pseudo-noise signals in a wide variety of circumstances.

The three sources of distortion in a multiple access system are thermal noise, clutter from authorized signals other than the desired talker, and jamming. The total interference power density is given by

$$N_{0T} = \left[N_0 W + \frac{KE}{T} + J \right] \frac{1}{W}. \tag{13}$$

The thermal noise power is given by N_0W where N_0 is the noise power density in watts per cycle per second and W is the bandwidth of the system. The clutter term is KE/T where K is the number of interfering signals at a given time, E is the energy of a single signal, which is assumed to be the same for all transmitted signals, and T is the duration of the signals. The jamming power is given by J.

Hence, the signal-to-noise ratio at the output of the matched filter is given by

$$\eta_p^2 = \frac{2E}{N_{0T}} = \frac{2E}{\frac{1}{W} \left[N_0 W + \frac{KE}{T} + J \right]},$$
 (14)

which assumes that the jamming signal looks like random

noise to the matched filter receiver. Special cases of operation arise when performance is limited in turn by each of the three causes of distortion. A thermal noise limited system would result in an output signal-to-noise ratio given by

$$\eta_p^2 = \frac{2E}{N_0}. (15)$$

This is the well-known result obtained by North⁷ and others.^{8,9} It is interesting to note that as is the case in standard point-to-point communication systems, the thermal noise is overcome by signal energy. In the clutter limited case, Eq. (14) reduces to

$$\eta_p^2 = 2W \frac{T}{K}. \tag{16}$$

Here, as expected, signal energy does not play a role in the performance of the system. This is true because increasing the signal energy for one user set means, according to our assumptions, that the energy would be increased for all in the same ratio and the ratio of received signal power to the received clutter power would not change. It is also interesting to note that the ratio of T/K can be considered as a constant of the system because an increase in the time duration of all signal waveforms results in a corresponding increase in the number of signals which are overlapping at a given time. The actual value of T/K is determined by the information flow of the entire multipleaccess system. Hence, we conclude that the only way to improve the output signal-to-noise ratio of all signals in a clutter-limited environment is to increase the bandwidth*. Finally, for the jammer limited case, Eq. (14) reduces to

$$\eta_p^2 = \frac{2WE}{I} = \frac{2WTS}{I} \,, \tag{17}$$

where S is the average signal power.

Here it is noted that the effectiveness of a white-noise jammer is reduced by a factor proportional to the matched filter processing gain (WT). However, a jammer could improve his effectiveness by repeating the signals he received, or by transmitting signals of the same form as those used by the system. This phenomenon is discussed in the following section.

Non-Gaussian capture model

The Gaussian noise model discussed in the previous section provides an explanation of the simulation results obtained when the clutter environment consisted of a set of signals of the same power as the desired signal. However, when the environment includes a dominant inter-

^{*} The effect of clutter on a particular signal may be reduced by an increase of its signal duration without changing the duration of other signals.

ference signal of greater average power than the desired signal, such as a clutter source, a CW jammer, or a repeater jammer, the Gaussian model does not offer a satisfactory explanation of the results. From the simulation results, it is seen that an interfering signal at twice the power of the desired signal causes a higher error rate than two interfering signals each equal in power to the desired signal.

The analysis presented in this section is based on the assumption that the rf phases of both the desired signal and the interference remain constant over a single rf pulse of each signal. The phase is uniformly distributed over the rf pulses. The basic matching process performed by the digital matched filter depends on constant rf phase over each pulse of the desired signal. A direct result of this assumption is that the receiver is captured by either the desired signal or the clutter source. Hence, in this case, capture probability is a more meaningful measure of performance than signal-to-noise ratio. In addition, both the analysis and simulation assume that the switching time for the biphase modulation is zero. However, it is conjectured that the results hold for nonzero switching times.

The environment considered in this section contains the desired signal $[A_1, \theta_1, \psi_1(t)]$ and an interference signal $[A_i, \theta_i, \psi_i(t)]$ with $A_i > A_1$ and no thermal noise. The outputs of the low-pass filter in the cosine and sine arms of the matched filter are, respectively

$$v_c = A_1 \cos \theta_1 \cos \psi_1(t)$$

 $+ A_i \cos \theta_i \cos \psi_i(t)$ (18a)

 $v_s = A_1 \sin \theta_1 \cos \psi_1(t)$

$$+ A_i \cos \theta_i \cos \psi_i(t)$$
. (18b)

First, consider the case of an interfering signal of greater power than the desired signal, and assume that

$$|\cos \theta_i| > |\cos \theta_1|. \tag{19}$$

When the inequality of Eq. (19) does not hold, the roles of the sine and cosine arms are reversed.

Since the output of an ideal hard limiter is the sign of the input, it follows that

$$v_{el} = \begin{cases} + \cos \psi_i(t) & \text{if } \cos \theta_i > 0 \\ - \cos \psi_i(t) & \text{if } \cos \theta_i < 0, \end{cases}$$
 (20)

where v_{el} is the output of the hard limiter in the cosine arm. In other words, the output in the cosine arm is independent of the desired signal.

From Eq. (18b) it follows immediately that the output of the hard limiter in the sine arm is

$$v_{*l} = \begin{cases} \pm \cos \psi_1(t) & \text{if } |A_1 \sin \theta_1| > |A_i \sin \theta_i| \\ \pm \cos \psi_i(t) & \text{if } |A_1 \sin \theta_1| < |A_i \sin \theta_i|, \end{cases}$$
(21)

Here, the output of the sine arm is determined by the desired signal if $(A_1 \sin \theta_1) > |A_i \sin \theta_i)$ and is determined by the interfering signal otherwise. (The equality of $|A_1 \sin \theta_1|$ and $|A_i \sin \theta_i|$ is neglected since it is a zero probability event.)

The problem of determining the probability that the interfering signal does not capture the system has now been reduced to determining the probability (P'_{\bullet}) that

$$A_1 \sin \theta_1 > A_i \sin \theta_i, \tag{22}$$

under the conditions

$$\sin \theta_1 > \sin \theta_i \tag{23}$$

and

$$A_i > A_1. \tag{24}$$

The absolute value symbol has been removed by restricting both phase angles to the range from zero to $\pi/2$. This restriction does not limit the generality of the results because $|\sin \theta|$ has the same distribution function over each range of $\pi/2$.

It is now a simple matter to obtain an upper bound on P'_c . The probability that Eq. (22) holds is certainly less than the probability that

$$A_1 > A_i \sin \theta_i. \tag{25}$$

Hence, since θ_i is assumed to be uniformly distributed over the range 0 to $\pi/2$,

$$\overline{P'_c} = 2/\pi \arcsin\left[\frac{A_1}{A_i}\right] \tag{26}$$

where $\overline{P_e^{\prime}}$ is an upper bound on the probability that the filter is not captured by the undesired signal. It is interesting to note that for a synchronized digital matched filter $(\theta_1 = \pi/2)$, Eq. (22) is replaced by Eq. (25) and, $P_e^{\prime} = \overline{P_e^{\prime}}$. At this point it is appropriate to assume that the signal is detected properly with probability one if it determines the output of either arm of the digital matched filter because the output of the detector is at least $2^{-1/2}$, and the simulation results have shown that the probability of noise producing an output exceeding $2^{-1/2}$ is extremely small.* The probability of correct detection is 1/M when the output is independent of the desired signal because all outputs are equally probable. Hence,

$$P_E = 1 - \left\{ 2/\pi \arcsin \frac{A_1}{A_i} + 1/M \left[1 - 2/\pi \arcsin \frac{A_1}{A_i} \right] \right\}, \qquad (27)$$

where P_E is the error probability for the M-ary "greatest of" detector. In the course of the simulation it was shown

[•] It was found that the output did not exceed 0.63 on any of the 150,000 trials used in determining the three standard distributions discussed.

that Eq. (27) is an excellent approximation to the error probability determined by the simulator.

Description of the simulation

The computer simulation of the digital matched filter was performed on an IBM 7094. The simulation model is described by the block diagram shown in Fig. 1. The principal aim of this simulation was to study the effects of clutter (from other users) on the error rate at the desired receiver. Thermal noise is neglected. Channel effects such as Doppler and multipath were also neglected. In addition it is assumed that the channel forms the composite signal by an algebraic summation of the desired and clutter signals.

All components in the receiver are assumed to perform their operations in an ideal manner. For instance there are no intermodulation terms in translating the input signal to if; the quadrature mixers introduce no distortion; there is no limiter ambiguity; etc.

The input signal to the receiver will contain the desired signal and K-1 undesired or clutter signals. Each of these K signals is of the form given in Eq. (1). Since ideal reception and quadrature detection are assumed, the simulation can work with the baseband quadrature components directly, thereby eliminating the need of generating the bandpass signal as part of the simulation. The inphase and quadrature components of the j^{th} clutter source are, respectively

$$v_{ej}(t-\Delta_i)=A_i\cos\psi_i(t-\Delta_i)\cos\theta_i,$$

and
$$v_{ej}(t-\Delta_i)=-A_i\cos\psi_i(t-\Delta_i)\sin\theta_i.$$
 (28)

The ensemble of signals is completely defined by the set of A_k , θ_k , ψ_k , and Δ_k . The delay Δ_k , relative to the delay of the desired signal, and the duty factor determine which signals overlap the desired signal and, hence affect the output at the time of match. The duty factor is given by $d = T/T_0$ where T is the duration of each pulse and $1/T_0$ is the repetition rate which is assumed to be the same for all signals. Although A_k and $\psi_k(t)$ are deterministic, the starting positions of the $v_k(t)$'s and their rf phases, θ_k , are considered as random variables. These starting positions and phase angles are assumed to be uniformly distributed over the ranges 0 to T_0 , and 0 to 2π , respectively. The rf phases are assumed to be constant over a pulse duration T.

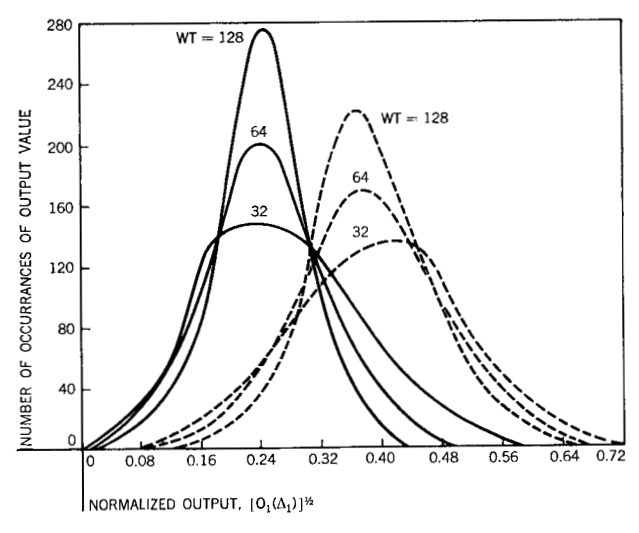
These composite signals, $v_c(t)$ and $v_s(t)$, comprised of partially overlapping signals given by Eq. (28) constitute the inputs to the demodulation simulator shown in Fig. 1.

The outputs of the limiters in the inphase and quadrature arms are sgn $\{v_c(t)\}$ and sgn $\{v_s(t)\}$ respectively, where

sgn (x) = 1 for x > 0, and sgn (x) = -1 for x < 0. The digital matched filter correlates the limited composite signal with the desired sequence given by $\cos \psi_1(t)$. Operationally, the output of the filter is the difference between the number of +1's and -1's in the sequence formed by the product of the sgn $\{v(t)\}$ sequence and the $\cos \psi_1(t)$ sequence. In both quadrature arms the results are then squared and summed. Finally, a normalizing factor is introduced to make the resulting range of values convenient for statistical analysis.

Perhaps the most important information provided by the simulation is the probability density function and cumulative distribution function of the output of the digital matched filter at the time of match. The time of match is the time at which the desired signal is fully loaded into the shift register. In the absence of thermal noise and clutter, it is the time at which the output of the digital matched filter is maximized. Also, of importance is the probability density function and cumulative distribution function at all times other than the time of match. It was expected that these functions are dependent on the processing gain* and that they are independent of the environment. These expectations were verified in the course of the simulation so that is was possible to use the same standard functions for all environments.

Figure 2 Distribution of normalized output signal values at instant of match. Solid curves indicate distributions with 30 partially overlapping signals and dashed curves, with 10. Signal processing gain (WT) is a parameter.



^{*} The processing gain equals the bandwidth-time product (WT) of the signals and is also equal to the number of bits in the shift register in each arm of the filter.

The distribution of the outputs at the time of match and at all other times is the raw data that is used to determine the probability of error for two kinds of detectors. First, consider the "greatest of" detector. The problem is to determine which of M positions is the time when the desired signal is matched. This is similar to the M-ary signal reception discussed in the literature. The "greatest of" detector is then a maximum likelihood detector. The probability of error P_E for this type of detector is

$$P_E = 1 - \sum_{\lambda=0}^{1} P_2(x_{\text{max},M} < \lambda) P_1(y = \lambda).$$
 (29)

Here, $P_2(x_{\max,M-1} < \lambda)$ represents the probability that the maximum of the M-1 values when the signal is not matched is less than λ and $P_1(y=\lambda)$ is the probability that the output at the time of match is equal to λ . The summation is over all the values of the output of the matched filter. The quantity $P_2(x_{\max,M-1} = \lambda)$ is calculated from repeated use of the recursion relation.

$$P_2(x_{\text{max},M-1} = \lambda) = P_2(x_{\text{max},M-2} < \lambda)P_2(x_1 = \lambda) + P_2(x_{\text{max},M-2} = \lambda)P_2(x_1 < \lambda),$$
(30)

where $P_2(x_1 = \lambda)$ is the probability that clutter will yield an output equal to λ . This probability is determined by a Monte-Carlo simulation.

Simulation results

In this section, some results of the simulation are tabulated. Figure 2 shows distribution functions for the matched filter output values at the instant of match when 10 and 30 signals overlap the desired signal for a variety of processing gains. The percent of overlap is chosen from a uniform distribution. Hence, the average overlap with the desired signal is 50%. If the average clutter power overlapping the desired signal is substituted into Eq. (10) the result agrees to within 10% with the result obtained from calculating $O_1(\Delta_1)$ from the data used to plot Fig. 2. The mean is also insensitive to the number of phase reversals per waveform for a specified number of clutter sources. For a given ratio of P_* to P_c one can also see that the distribution is more peaked for higher WT products, as would be expected.

Figures 3 and 4 illustrate the probability of error for a "greatest of" detector as a function of the number of equal-power talkers (signals) per megacycle. The "greatest of" detector makes a decision that the signal is matched in the time slot for which the receiver output is greatest. In fact the signal is matched, although masked by clutter, in one of the M time slots considered by the detector. In these figures and those that follow it was assumed that each talker transmitted 8000 signals per second and each biphase bit is of 0.2 μ sec, duration. Hence, the

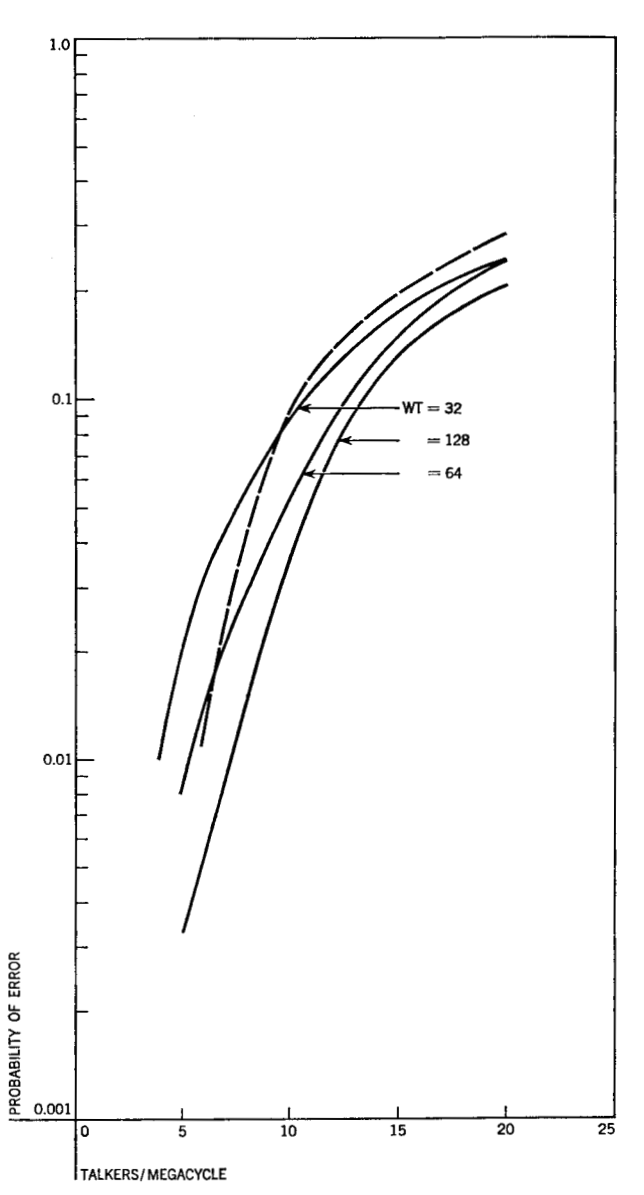


Figure 3 Error rate vs number of equal-power talkers per megacycle using "greatest of" detection with M=8 quantization levels. Signal processing gain is a parameter. Dashed curve derived from Turin's results for analog matched filters.

duty factor for each user is 0.2, 0.1, 0.05 for 128, 64 and 32 bit digital matched filters, respectively.

Figure 5 gives another presentation of error rate curves as functions of the number of equal-power talkers per megacycle, where WT is held constant at 128 and the number of quantization levels, M, is allowed to vary.

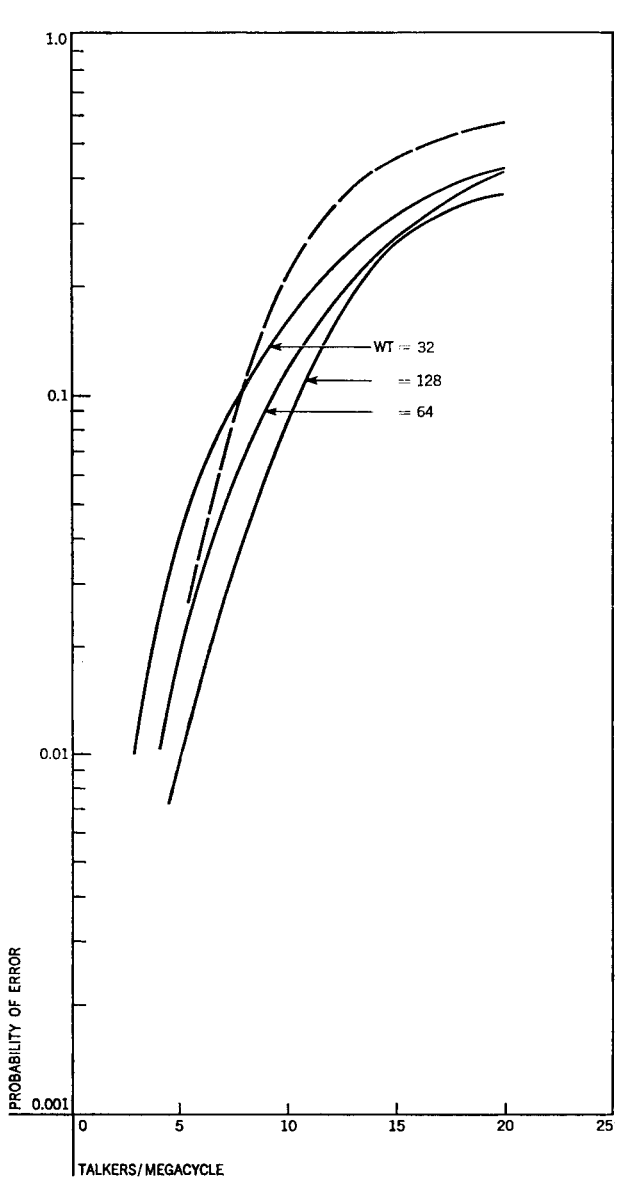


Figure 4 Error rate vs number of equal-power talkers per megacycle using "greatest of" detection with M=32 quantization levels. Signal processing gain is a parameter. Dashed curve from Turin.

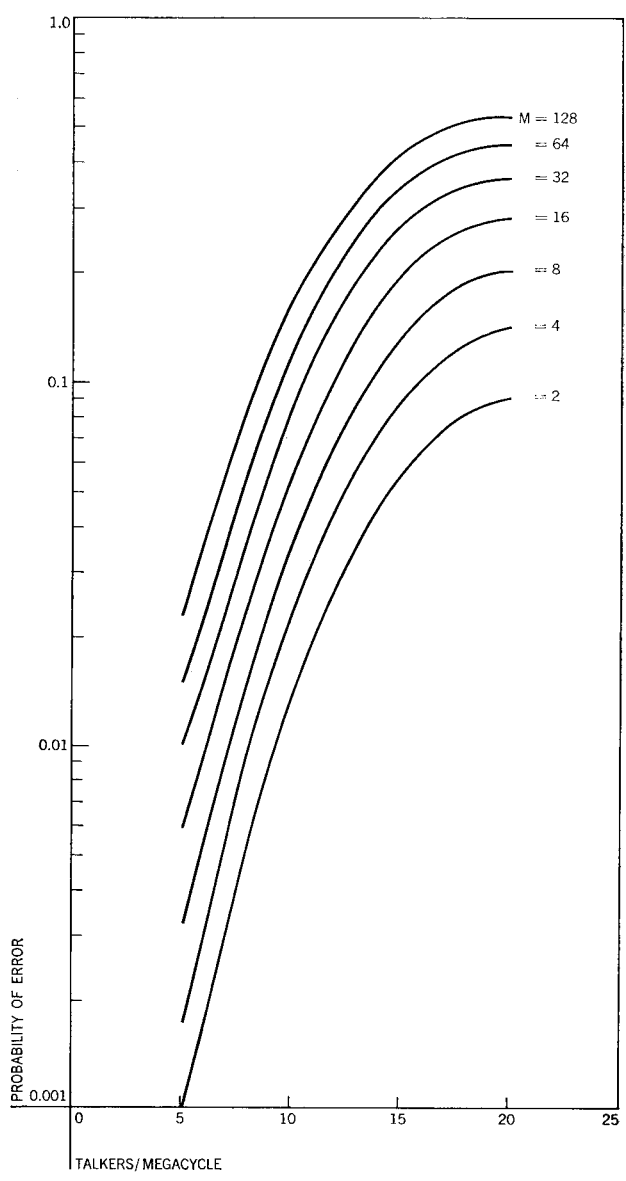


Figure 5 Error rate vs number of equal-power talkers per megacycle using "greatest of" detection with WT=128. Number of quantization levels is a parameter.

Figures 6 and 7 illustrate the effect of one strong talker on the performance of the system. The strong talker is received with a 60 dB power advantage over the desired talker so that when the strong talker's signal is present the receiver matches to his signal. The limiting performed by the receiver is ideal hard limiting and spill-over in time and frequency is neglected. These curves indicate the error rate when the strong talker partially overlaps

the desired talker with probability one. Since the strong talker and desired talker are not in time synchronism, the overlap is chosen from a uniform distribution from zero to total overlap. These figures also show the effect of the duty factor when the system contains a strong talker. These curves were plotted by weighting the strong-talker curves by the probability that the strong talker overlaps the desired talker and by weighting the equal power talker

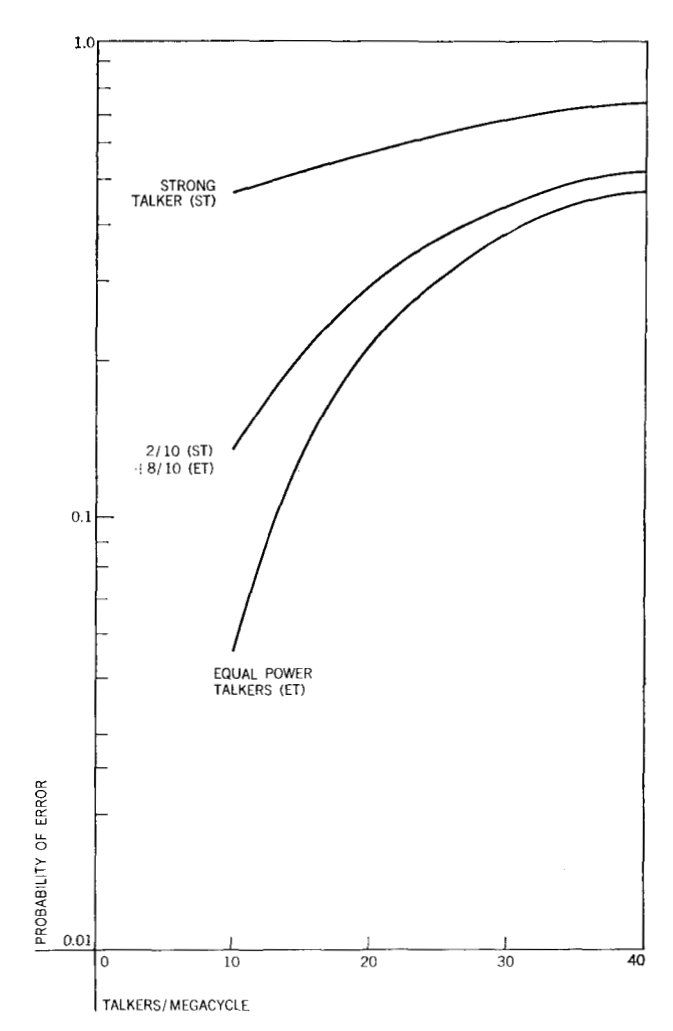


Figure 6 Effects of one "strong talker" on error rate. "Greatest of" detection; 8 quantization levels; signal processing gain, WT=64.

curves by the probability that the strong talker does not overlap the desired talker.

Up until now, we have considered only the case where we know that the signal will be present and that it will be in one of M different time slots, thereby allowing the use of "greatest of" detection. However, the case where signal synchronization is not desired or possible is also of considerable interest. Here, a threshold type detector must be employed. Figure 8 gives curves of probability of false detection as a function of probability of false alarm for various talker per megacycle values, with threshold detection.

The previously presented data have been limited to either very strong talkers or equal-power talkers. Figure 9 shows results for a "greatest of" detector in an environment consisting of the desired signal and one clutter source of greater power that completely overlaps the desired

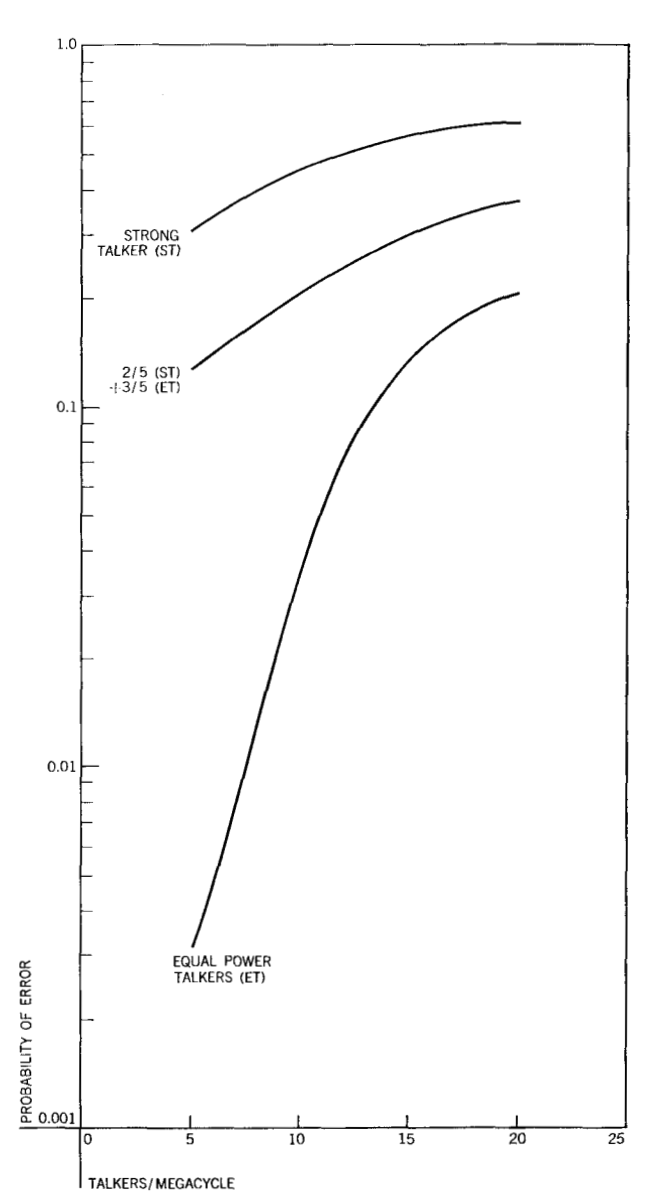


Figure 7 Effects of one "strong talker" on error rate. "Greatest of" detection; 8 quantization levels; signal processing gain, WT = 128.

signal. The simulation results are also compared against Eq. (27). For this case the simulation results were independent of WT as discussed earlier.

Figure 10 gives results using "greatest of" detection for sets of clutter talkers whose powers vary in a particular manner. The talkers are distributed such that the desired talker is a distance A, and the nearest talker is a distance $B \le A$ from the receiver. The remaining talkers are distributed uniformly over the area contained between the concentric circles whose centers are at the receiver and whose radii are A and B. The received power is assumed to vary inversely with the fourth power of the

distance between the transmitter and receiver. An equal number of additional talkers is distributed uniformly between concentric circles whose centers are at the receiver and whose radii are A and 2A. (These talkers do not count in computing the talkers per megacycle.) An important conclusion that follows from Figures 9 and 10 is that the error rate increases at a faster rate with increasing dynamic range than would be predicted from a Gaussian noise model.

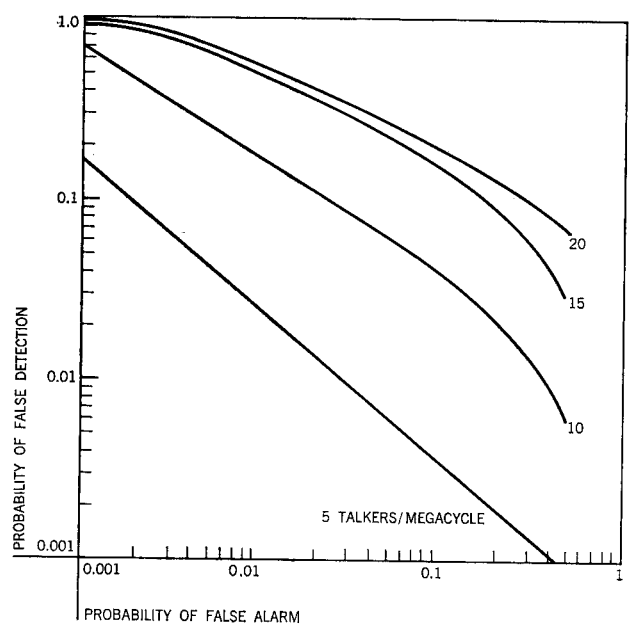
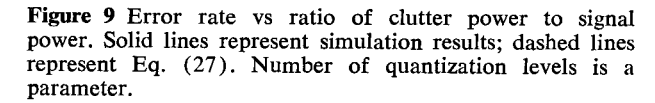
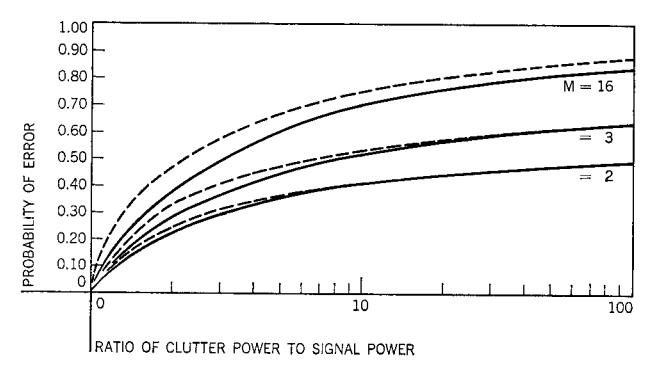


Figure 8 Probability of false alarm vs probability of false detection for various numbers of talkers per megacycle. Threshold detection.





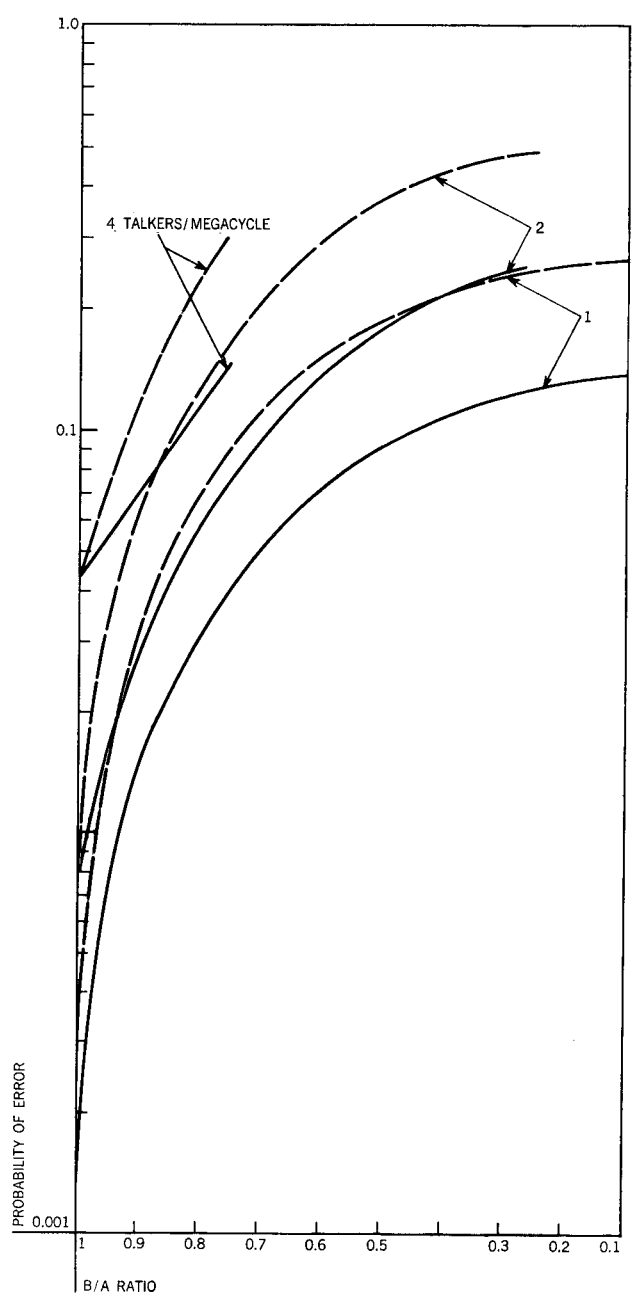


Figure 10 Effects of distributed-power talkers on error rate. "Greatest of" detection; 32 quantization levels; and signal processing gain, WT=64. Solid lines: unequal-power talkers uniformly distributed between distances B and A from receiver. Dashed lines: equal-power talkers at B.

References

- F. P. Corr, R. Crutchfield and J. Marchese, "A Pulsed Pseudo-Noise VHF Radio Set," *IBM Journal* 9, 256-263 (1965).
- G. L. Turin, "An Introduction to Matched Filters," IRE Trans. on Information Theory IT-6, 311-329 (1960). The issue of the Transactions in which this article appears also contains other pertinent papers on analog matched filters.

- 3. G. L. Turin, "The Asymptotic Behavior of Ideal M-ary
- Systems," *Proc. IRE*, 47, 93-94 (1959).
 4. S. Reiger, "Error Rates in Data Transmission," *Proc. IRE* 46, 919-920 (1958).
- 5. A. H. Nuttall, "Error Probabilities for Equicorrelated M-ary Signals Under Phase-Coherent and Phase-Incoherent Reception," IRE Trans. on Information Theory IT-8, 305-314 (1962).
- 6. J. W. Goodman, et al., "Some Signal Suppression Properties of Ideal Limiters," AF 33(616)-7944, Project No. 4036, Task No. 403603, ASO, WPAFB, AD 299070 (November,
- 7. D. O. North, "An Analysis of the Factors Which Determine Signal/Noise Discrimination in Pulsed-Carrier Systems," RCA Laboratories, Princeton, N. J., Report PTR-6C (June,
- 8. J. Van Vleck and D. Middleton, "A Theoretical Comparison of the Visual, Aural, and Meter Reception of Pulsed Signals in the Presence of Noise," *Jour. Appl. Physics* 17, 940–971 (1946).
- 9. B. M. Dwork, "Detection of a Pulse Superimposed on Fluctuation Noise," Proc. IRE 38, 771-774 (1950).

Received April 20, 1965.